Reaction Control in Bacteriorhodopsin: Impact of Arg82 and Asp85 on the Fast Retinal Isomerization, Studied in the Second Site Revertant Arg82Ala/Gly231Cys and Various Purple and Blue Forms of Bacteriorhodopsin

Karsten Heyne, Johannes Herbst, Barbara Dominguez-Herradon, Ulrike Alexiev,* and Rolf Diller*

Institut für Experimentalphysik, Freie Universität Berlin, Arnimallee 14, 14195 Berlin, Germany

Received: August 13, 1999; In Final Form: March 9, 2000

Femtosecond time-resolved optical absorption experiments reveal that the changes of the excited electronic state dynamics observed between bacteriorhodopsin wild type and the single mutant R82A are completely reversed in the double mutant R82A/G231C. Thus, the bacteriorhodopsin double mutant R82A/G231C is shown to be a second site revertant with respect to the primary ultrafast all-trans to 13-cis photoisomerization of the retinal cofactor. The results imply that in R82A/G231C a cofactor binding pocket is realized in which, at physiological pH, the arginine residue in position 82 (R82) is not, but a deprotonated D85 is needed for a wild-type-like fast retinal photoisomerization. The revertancy found for R82A/G231C and further results on the single mutants R82A, R82C, R82Q, and G231C at various pH values and ion concentrations confirm and broaden the range of applicability of the known correlation between the protonation state of aspartic acid 85 (D85) and the time constants of the excited electronic state decay. Among the bR mutant systems investigated, species with D85 deprotonated exhibit an excited electronic state decay time constant of $\tau_1 = 0.52 \pm 0.05$ ps whereas systems with D85 protonated show a biphasic decay with $\tau_1 = 1.7 \pm 0.3$ and τ_2 ranging from 6 to 12 ps. It is noted that the distribution of the τ_2 times is much wider than that of the τ_1 times.

Introduction

A common feature of a number of extremely biologically important retinal proteins is the ultrafast photoinduced isomerization of the retinal cofactor around one of its C=C double bonds. Prominent examples are the proton pump bacteriorhodopsin (bR), visual rhodopsin, and the chloride pump halorhodopsin.[1] Among them, bR is the system which has been investigated most extensively. It is a transmembrane protein in the plasma membrane of *Halobacterium salinarium* and contains a retinal chromophore which is covalently bound to K216 via a protonated Schiff base.[2−4] The primary all-trans to 13-cis photoisomerization of the retinal cofactor initiates a photocycle that is accompanied by an efficient proton transfer across the cell membrane and enables ATP production and thus survival of the organism at low oxygen concentration. After photoexcitation of the ground state BR_{570} (the index denotes the absorption maximum) with the cofactor in its all-trans configuration, the 13-cis electronic ground state (J) is reached after 0.5 ps[5,6] with a quantum yield of 64%.[7−9] Further relaxation processes, probably vibrational and torsional relaxation,[10−13] lead to the K-state within 3 ps, which stays more or less stable for hundreds of nanoseconds. Deprotonation and subsequent reprotonation of the Schiff base nitrogen[14−16] as part of the proton pump process occur in bR wild type (wt) not until the microsecond−millisecond time regime.

Recently, on the basis of femtosecond transient absorption experiments,[17−20] the question was raised again as to when the primary isomerization in bR takes place with respect to the decay of the excited electronic state (ESD). This issue is not the subject of this paper, yet the ESD time is taken as a significant measure of the isomerization process.

From comparison of these biological systems with the photoinduced isomerization dynamics of all-trans retinal (as protonated Schiff base) in solution,[21] it must be concluded that the specificity of the protein-based isomerization is determined by the constituents forming the chromophore binding pocket, i.e., amino acid residues with varying chemical and physical properties such as size and electrical charge. The specificity of the isomerization concerns the affected C=C bond, the rate constant as measured, e.g., by the retinal excited state lifetime, and the quantum yields for reactive and nonreactive pathways. The binding pocket forces the retinal cofactor into a new static equilibrium geometry as compared to its structure in solution, thereby modifying the electronic potential energy surfaces and thus the reactivity of the cofactor. Charged amino acid residues as part of the binding pocket play an important role in this respect. In the case of bR this concerns especially the aspartic acids 85 and 212 and arginine 82. This was demonstrated by Kobayashi[22] and co-workers and El-Sayed[23] and co-workers, who showed that the excited electronic state decay slows significantly when turning bR wt into its blue form or when replacing charged amino acid residues in the binding pocket with neutral ones. It was concluded from these experiments that the protonation state of D85, more specifically the negatively charged form of D85, catalyzes the decay rate of the excited state. ESD times of 0.5 ps were found for bR wt and mutant proteins bearing the deprotonated form of D85. bR wt and mutant proteins with a protonated D85 showed two ESD components with time constants of 1.5 and ≈10 ps, respectively.

* To whom correspondence should be addressed. E-mail: diller@physik.fu-berlin.de; alexiev@physik.fu-berlin.de.

10.1021/jp992877u CCC: $19.00
Published on Web 06/01/2000

In this report we have further tested the catalytic function of D85 for the ESD decay in a set of bR mutant proteins, which contain a point mutation in the retinal binding pocket in position 82. The mutation R82A leads, as expected from earlier results with R82Q,[23] to a slowdown of the excited-state decay due to a rise of the pK_a of D85 from about 2 to 7.[24] Mutation of charged amino acids in the retinal binding pocket often leads to drastically disturbed photocycle and proton pumping characteristics as shown for example for D85N, R82Q, R82A, and D212N.[25] Our set of R82 mutant proteins contains a double mutant in which the characteristics of the R82A single mutant, namely accelerated kinetics of Schiff base deprotonation, reversed order of proton release and uptake, and the pK_a of D85, are fully restored to wt-like behavior when adding the mutation G231C on the cytoplasmic surface of the protein, far away from the retinal binding pocket.[26]

With this second site revertant, containing a modified binding pocket with a reduced "diffuse counterion" (D212, D85) compared to wt (D212, D85, R82), we have the opportunity to test three points: first, to test whether this mutant protein is also a second site revertant on the time scale of the photoinduced isomerization dynamics using optical transient absorption spectroscopy, second, to confirm the catalytic role of D85, and third, to further elucidate the role of charged amino acids in the binding pocket. We follow the strategy of the determination of a minimal set of critical parameters that suffices to enable the wt-like isomerization features. This set of critical parameters includes the essential spatial charge distribution in the close vicinity of the cofactor, realized by a minimal number of charged amino acid residues at specific locations with respect to the cofactor. Since the spatial charge distribution also depends strongly on pH and ion concentration, we have studied in addition the excited electronic state decay of various bR mutant samples, concentrating on position 82.

Materials and Methods

Purple membranes of bR wt were isolated from the *Halobacterium salinarium* strain ET1001. Bacteriorhodopsin single mutants R82A, R82Q, R82C, G231C, and the double mutant R82A/G231C were expressed in *H. salinarium*. In the mutant proteins R82A, R82Q and R82C, alanine, glutamine, and cysteine, respectively, replace arginine in position 82, and in G231C cysteine replaces glycine in position 231. Preparation, expression, and isolation procedures were described in the literature.[27,28] For the transient absorption measurements the samples were set to 15 mM KCl, unless otherwise stated, and the pH was adjusted by various buffers: pH 7 by 1 mM Tris (Sigma), pH 2.7−5.8 by 1 mM sodium acetate, and pH 9−11 by 1−3 mM potassium carbonate buffer. The deionized samples were prepared by gel chromatography using prefilled AG50W-X4 columns (Biorad). The pH of the deionized samples is ≈5. In addition, the R82C mutant was incubated with an equimolar amount of Hg^{2+} ions leading to a binding of the Hg^{2+} ions to the thiol group of the cysteine moiety in position 82.[29] In the following this sample is denoted as R82C−Hg^+. A summary of the various samples including specific important properties are listed in Tables 1 and 2. Based on the respective pK_a values of the purple-to-blue-transition given in refs 26 and 29, the experimental conditions were chosen such that the various mutant proteins are either in the blue form with $\lambda_{max} \approx 600$ nm or in the purple form with $\lambda_{max} \approx 570$ nm, at the pH values indicated. The pK_a values at 150 mM KCl are 2.6, 2.7, and 2.1 for wt, G231C, and R82A/G231C,[26] respectively, and only slightly higher in 15 mM KCl. For R82A, R82C, and R82C−Hg^+ the pK_a values in 15 mM KCl are 8.1, 7.4, and 6.5, respectively.[29]

TABLE 1: List of the Purple bR Forms (λ_{max} at about 570 nm), Experimental Parameters as pH, λ_{max} (Light Adapted), and Fit Results of the Kinetic Data (Decay Times τ_1, τ_2 and Respective, Normalized Amplitudes A_1, A_2)[a]

sample	pH	λ_{max}/nm	τ_1/ps	τ_2/ps	A_1	A_2
wt	7.0	568	0.55(5)		1.0	
wt	10.0	568	0.53(5)		1.0	
R82A/G213C	7.0	567	0.57(5)		1.0	
R82A/G213C	10.0	567	0.54(5)		1.0	
G231C	7.0	568	0.57(5)		1.0	
R82C	10.0	565	0.48(5)	4.9(1.0)	0.83(2)	0.17(2)
R82Q	10.0	560	0.43(5)	2.5(6)	0.85(2)	0.15(3)
R82A	10.0	562	0.51(5)		1.0	

[a] All samples are in 15 mM KCl. Errors given in parentheses refer to the last digit(s).

TABLE 2: List of the Blue bR Forms (λ_{max} at about 600 nm), Experimental Parameters as pH, λ_{max} and Fit Results of the Kinetic Data (Decay Times τ_1, τ_2 and Respective, Normalized Amplitudes A_1, A_2)[a]

sample	pH	λ_{max}/nm	τ_1/ps	τ_2/ps	A_1	A_2
R82A	7.0	≈600	1.7(2)	6.4(8)	0.66(5)	0.34(5)
R82A	5.8	≈600	1.7(3)	6.4(1.2)	0.64(9)	0.36(10)
R82C	7.0	585	1.8(2)	12.4(9)	0.57(3)	0.43(3)
R82C	5.8	≈590	1.5(2)	8.4(9)	0.59(5)	0.41(5)
R82C−Hg^+	5.8	585	1.4(2)	8.3(8)	0.59(4)	0.41(4)
wt	2.7	603	1.8(5)	12(3)	0.51(4)	0.49(4)
R82A/G231C	2.7	602	[2.5(6)]	[21.8(7.3)]	0.66(11)	0.34(9)
wt-deion.	≈5	602	1.9(3)	11.8(7)	0.53(2)	0.47(2)
R82A/G231C-deion.	≈5	602	1.8(2)	12.4(8)	0.49(1)	0.51(1)

[a] All samples are in 15 mM KCl except deionized samples. Errors given in parentheses refer to the last digit(s). Values in square brackets are not part of quantitative discussion due to the large experimental error.

The transient absorption experiments were performed by means of a pump/probe spectrometer, based on a titanium−sapphire CPA-laser system (Clark). Excitation pulses at 570 nm and probe pulses were extracted from a white light continuum at a repetition rate of 1 kHz, providing an instrumental response function of typically 450 fs. Signal processing was performed by lock-in detection of the photodiode signals at 1 and 0.5 kHz at the same time. The spectrally broad band probe beam was superimposed with the pump beam (both focused) in the sample and then fed into a monochromator to spectrally resolve the transient absorption signals. The samples consist of aqueous suspensions of "purple membrane" patches between two calcium fluoride windows with a spacing of 1 mm. The term "purple membrane" refers to the membrane fragments that contain bR and occur naturally in *H. salinarium* and should not be confused with the term "purple form" used later in this paper. The sample was rotated and moved back and forth transversely to the laser beams during the experiment in order to guarantee sample being in the initial state at each laser shot. Care was taken to provide for light-adapted bR and, in cases of slow photocycle completion, to impede the accumulation of long-living intermediates in the sample cell that could contribute to the absorption signals. The experiments were performed at room temperature. At each probe wavelength kinetics of the various samples were taken immediately after each other in order to ensure identical experimental conditions. Thus, a high relative accuracy of the extracted decay times was obtained.

Kinetics were taken at probe wavelengths in the spectral range between 420 and 760 nm and at 900 nm. From the kinetics, transient absorption difference spectra were derived for various

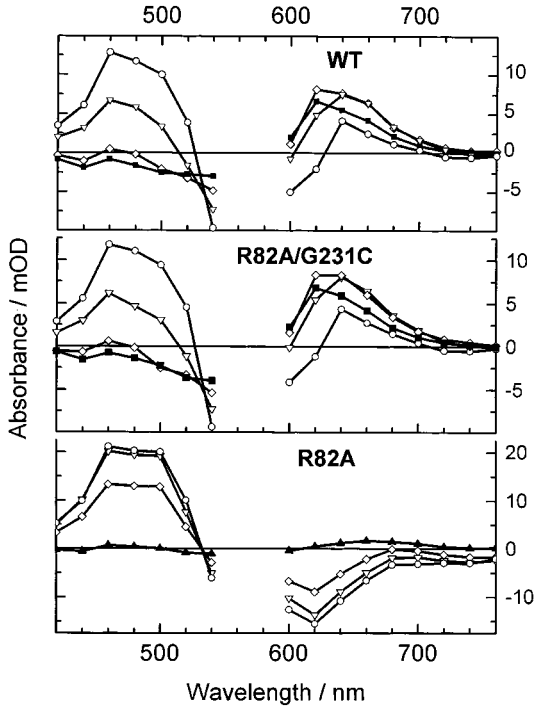

Figure 1. Transient absorption difference spectra of bR wild type (wt) and the mutants R82A/G231C and R82A at delay times of 0.5 ps (open circle), 1.0 ps (open down triangle), 2.0 ps (open diamond), 15.0 ps (solid square; wt and R82A/G231C), and 18.0 ps (solid up triangle; R82A). The gap at 560 and 580 nm is due to the excitation wavelength at 570 nm. All spectra were taken at pH 7.

delay times. The kinetic traces taken at 480 nm (region of basically solely excited-state absorption) were analyzed by a least-squares fitting routine assuming a sum of exponentials with respective amplitudes and decay time constants, including the convolution with the system response function. In Tables 1 and 2 for each sample up to two significant decay components are given with τ_1 and τ_2 being the shorter and longer decay time, respectively.

Results

It is known that a change of the charge distribution in the binding pocket of the retinal cofactor has a strong impact on the decay of the excited electronic state. Mutations at position 85, 212, and 82 that remove charges slow the excited-state decay.[23] This effect was correlated[22,23] with the protonation of D85 and is confirmed in our experiments for R82A and other 82 mutants. The pK_a of D85 controls the purple-to-blue-transition in bR.[24,30] Therefore the λ_{max} value of the chromophore can be taken as a measure of the protonation state of D85, with blue a protonated D85 and purple a deprotonated D85.

Figure 1 shows absorption difference spectra in the region between 420 and 760 nm at various delay times of bR wt, the single mutant R82A, and the double mutant R82A/G231C at neutral pH and 15 mM KCl at room temperature. The difference spectra demonstrate first the spectral characteristics of the molecular species generated within the first 15 ps (18 ps, respectively) after photoexcitation, second their changes with respect to wt that occur in the single mutant R82A, and finally the restoration of wt behavior in the double mutant R82A/G231C. The spectra are dominated by the bleach of the electronic ground state absorption band (≈520−640 nm), the absorption band of the excited state (420−540 nm), and the photoproduct absorption band (600−700 nm). Bleach and

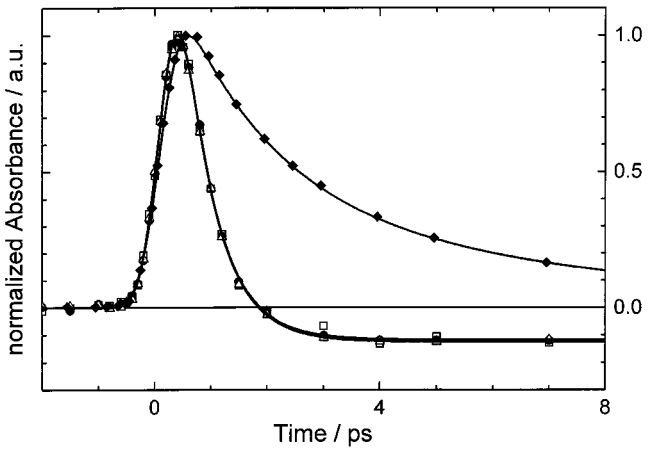

Figure 2. Transient absorption difference signals of bR wt (solid circle), G231C (open up triangle), R82A/G231C (open square), and R82A (solid diamond) at probe wavelength 480 nm in the region of the excited-state absorption. All transients were taken at pH 7. Shown are the experimental data points and fits according to the parameters given in Tables 1 and 2.

excited-state spectra rise with the exciting laser pulse. As the excited state decays (Figure 2), the product absorption bands rise and become stationary on the time scale of the experiment (up to 40 ps).

Clearly, although the transient difference spectra of R82A show major differences as compared to those of wt as expected from the different protonation state of D85 in the respective samples, the difference spectra of wt and R82A/G231C and G231C (not shown) are indistinguishable from each other within the experimental error. The transient spectral features of wt are reestablished when adding the mutation G231C to R82A. This rescue of wt behavior in the double mutant is demonstrated equally well in the kinetics at 480 nm of wt, R82A, G231C, and R82A/G231C (all at pH 7) as shown in Figure 2. Similar results were obtained in the spectral region of stimulated emission at 900 nm (data not shown). This behavior follows the correlation found for the protonation state of D85 and the ESD times.[22,23] In R82A at pH 7 a protonated D85 leads to a slowdown of the ESD, whereas in the double mutant R82A/G231C with a deprotonated D85[26] at pH 7 the time constants are wt-like (cp. Table 1).

In particular, the excited-state decay of the double mutant R82A/G231C coincides very accurately with that of bR wt. It should be pointed out that, from the quantitative match of the transient wt difference spectra with those of R82A/G231C (ratio of maximal excited-state amplitude at 480 nm and final product state amplitude at 620 nm), it follows that the all-trans to 13-cis isomerization quantum yield of R82A/G231C is the same as that of bR wt, namely about 64%. From the extreme similarity among the kinetic data described above, it can be concluded that the primary trans−cis photoisomerization dynamics of the retinal cofactor in R82A/G231C is the same as that in bR wt.

To further characterize the second site revertant R82A/G231C and to learn more about the role of charges for the fast photoisomerization, we have varied parameters such as pH or ion concentration in parallel for the single mutants R82A and G231C and the double mutant R82A/G231C. To test the specific sterical effect of the positive charge at position 82 we have used the mutant R82C, where the positive charge can be reestablished by adding Hg^{2+} ions (R82C−Hg^{+}) although not exactly in the sterical position as in wt. The specific experimental conditions (pH, ion concentration) or modifications (R82C−Hg^{+}) are listed in Tables 1 and 2. In Figures 2−4, transient absorption signals

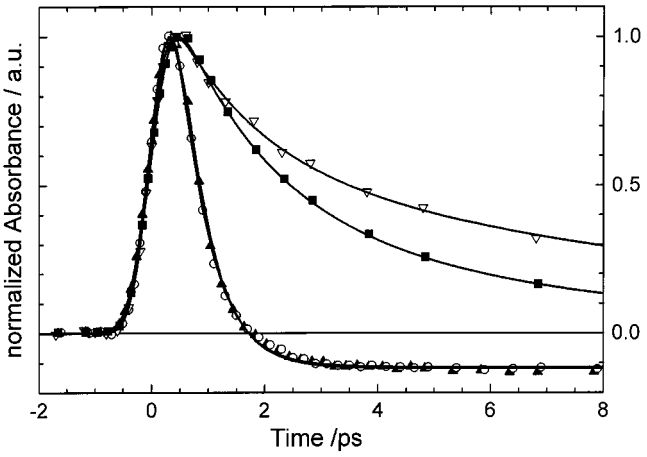

Figure 3. Transient absorption difference signals of bR wt pH 10.0 (open circle), R82A pH 10.0 (solid up triangle), wild type pH 2.7 (open down triangle), and R82A pH 7.0 (solid square), taken at 480 nm. Shown are the experimental data points and fits according to the parameters given in Tables 1 and 2.

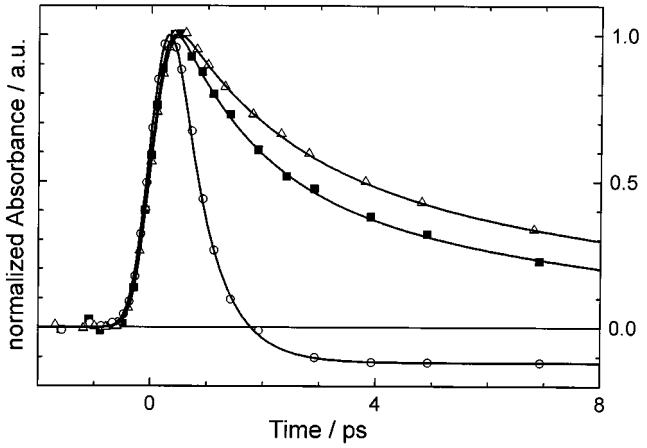

Figure 4. Transient absorption difference signals of bR wt at pH (open circle), wt deionized (open triangle), and R82C-Hg^+ (solid square) at probe wavelength 480 nm. Shown are the experimental data points and fits according to the parameters given in Tables 1 and 2.

at 480 nm of the various samples are shown together with their respective least-squares fits according to the parameters given in Tables 1 and 2. In this spectral region the signals are due almost solely to the electronic excited state absorption (cp. Figure 1); i.e., they do not carry contributions of other states as the electronic ground state or product states. Thus, the signal decay at 480 nm is taken as a measure of the decay of the electronic excited state to an electronic ground state.

In Figures 2 and 3, kinetics of bR wt, R82A, G231C, and R82A/G231C at different pH values are shown. All signals show a fast rise, determined by the width of the exciting laser pulse, and a fast decay in the case of wt (pH 7 and 10), G231C (pH 7), R82A/G231C (pH 7), and R82A (pH 10). The signals level at long delay times at a small negative absorbance amplitude, due to the ground state bleach signal with peak at about 570 nm. The signals of R82A (pH 7) and wt (pH 2.7) show a substantially prolonged decay. The kinetics shown in Figures 2 and 3 were chosen as representatives of samples with a deprotonated D85 with an absorption maximum of 570 nm (purple forms, fast decay) and of samples with a protonated D85 with an absorption maximum at about 600 nm (blue forms, slow decay). In Tables 1 and 2 the results of the excited state decay analysis of the purple and blue forms, respectively, are given. They can be summarized as follows.

Purple Forms. Wt, R82A/G231C, and G231C are purple forms at pH 7. In addition to this, R82A, R82C, and R82Q turn to purple forms at pH 10 (cp. Materials and Methods). All purple forms are characterized by a short excited state decay time τ_1 in the range between 0.43 and 0.57 ps with a large amplitude. The τ_1 values exhibit a remarkable reproducibility (see Table 1); i.e., within the experimental error of 0.05 ps around the mean value of 0.52 ps no differences were found for the fast excited state decay kinetics. A second excited state decay component (with small amplitude) is observed only for R82Q (pH 10.0) and R82C (pH 10.0) with decay times τ_2 of 2.5 $\pm$ 0.6 and 4.9 $\pm$ 1.0 ps, respectively.

Blue Forms. R82A and R82C are blue forms at or near neutral pH (5.8 and 7) at the low salt conditions used in the experiment. Furthermore, wt and R82A/G231C are blue forms at acid pH (2.7) and as deionized samples. The excited-state decay of all blue forms is biphasic with the same short decay time τ_1 of 1.7 $\pm$ 0.3 ps and the longer decay time τ_2 found roughly between 6 and 12 ps. It is noted that, in contrast to τ_1, the value of τ_2 varies much more, i.e., for a factor of about 2. The shorter decay time τ_1 is significantly longer than the decay time τ_1 of the purple forms. Wt at pH 2.7, wt deionized, and R82A/G231C deionized show the same excited state decay times τ_2 within the experimental error (12 $\pm$ 3, 11.8 $\pm$ 0.7, 12.4 $\pm$ 0.8 ps, respectively). The excited state of R82A decays with the shortest τ_2 of all blue forms investigated, i.e., 6.4 $\pm$ 1.2 ps. R82C at pH 7.0 and pH 5.8 has longer τ_2 of 12.4 $\pm$ 0.9 ps and 8.4 $\pm$ 0.9 ps, respectively.

As shown in Figure 2 the excited state decay time slows when the positive charge at position 82 is removed in R82A (1.7 ps). The same effect is observed in R82C, which is a blue form near neutral pH (5.8 and 7) and exhibits similar decay times τ_1 (1.5 and 1.8 ps). The positive charge at position 82 can be reinserted as in R82C$-Hg^+$ (cp. Materials and Methods). However, R82C$-Hg^+$ still shows a "long" τ_1 of 1.4 $\pm$ 0.2 ps. In Figure 4 the kinetics of R82C$-Hg^+$ (pH 5.8) and, for comparison, a blue (deionized) and a purple form (pH 7) of wt are shown. They all are positively charged at position 82 but exhibit significantly different decay times τ_1, i.e., 1.4 ps (R82C$-Hg^+$, blue form) and 1.9 ps (wt deionized, blue form) and 0.55 ps (wt, purple form).

Discussion

Tables 1 and 2 show a strong correlation between the protonation state of D85 as indicated by the specific pK_a or the absorption maximum of the purple forms (between 562 and 568 nm) and the blue forms (between 585 and 605 nm), respectively, and the occurrence of either 0.5 or 1.7 ps as the shorter observed ESD time (τ_1). Thus, the catalytic impact of the charge of D85 on the ESD kinetics[22,23] applies as well for the double mutant R82A/G231C and the other single mutant systems studied. The mechanism that facilitates this correlation is found in the physical interaction between the retinal cofactor and the charge on D85 which itself is determined by the specific chemical boundary conditions in the cofactor binding pocket. In principle, the potential energy surfaces of the cofactor electronic states participating in the isomerization can be constructed from the free retinal electronic states and the three-dimensional protein structure.[31,32] More specifically, it can be argued[23,33] that a negative charge positioned in a distance of a few angstroms from the retinal polyene chain interacts locally with the more or less delocalized π-electron system. In a system with a protonated Schiff base like bR, the positive charge on the retinal cofactor can be stabilized at a specific position on the polyene

chain by a suitably positioned negative charge. Thus, the counterion stabilizes a specific ground-state conformer of the molecule, e.g., the all-trans form in the case of the protein bound retinal in bR, with respect to thermal isomerization but increases the rate of photoisomerization around a specific C=C double bond, e.g., the C_{13}=C_{14} double bond in bR. According to this model, a change of the charge distribution in the cofactor binding pocket is expected to alter the C−C bond order and the isomerization dynamics. The charges in the cofactor binding pocket in the unphotolyzed bR at neutral pH (bR_{570}) are mainly given by the negatively charged aspartic acids D85 and D212[34] and the positively charged arginine R82.[35] It was shown[22,23] and is confirmed by our results on the single and double mutants that the charge on D85 is the dominant counterion with respect to the ESD catalysis.

Moreover, the results on the double mutant R82A/G231C demonstrate that the correlation between a deprotonated D85 and a short ESD time is realized at physiological pH even in a binding pocket with a substantially altered charge distribution as compared to bR wt, i.e., the missing R82. As is known, the pK_a of D85 can be strongly influenced by parameters of the binding pocket, e.g., the spatial distribution of charges, water molecules, and other polarizable groups. In the single mutant R82A such a change in the charge distribution is realized by mutation and an increase of the pK_a of D85 is observed.[24] In the double mutant R82A/G231C we now have the interesting situation that the second mutation (G231C), which alters the pK_a of D85 back to a wt-like value, is not located in the binding pocket itself. We must conclude that in the double mutant the crucial microenvironment, necessary for a wt-like pK_a of D85 and a short ESD time τ_1, is reestablished. The underlying mechanism must include the displacement of charges or of partial charges of polarizable groups within the cofactor binding pocket. Groups involved in this process are for example the side chains of the amino acids D85, D212, R82, Y185, Y57, and T89 that are part of a hydrogen bond network involving furthermore the retinal Schiff base proton and water molecules. This network is revealed by the structural data available on bR.[36−38] Note that a deprotonated Schiff base in the unphotolyzed state of R82A/G231C can be ruled out since in this case a strong blue shift of the pigment λ_{max} as in the intermediate state M_{410} is expected but is not observed.

Based on the analysis of the ground state absorption spectra, photocycle kinetics, and kinetics of proton release and uptake in the mutants R82A and R82A/G231C, a model is presented in ref 26 giving a rationale for such a displacement of charges. This model explains the observed rescue effects in R82A/G231C with the rearrangement of the native hydrogen bonded network connected with D212, leading to an equivalent hydrogen bonded network as in wt and facilitating proton release to the extracellular surface without the participation of D212 and R82. Indeed, D212 is the only charged residue in the microenvironment of the bR_{570} cofactor of R82A/G231C besides D85. In a simplistic hypothesis, the charges of R82 and D212 compensate each other in wt. In R82A the positive charge R82 is removed and the negative charge of D212 remains effective and increases the pK_a of D85. In R82A/G231C the negative charge of D212 is ineffective (e.g., by shielding or conformational change) and the pK_a of D85 is reduced, enabling the fast (0.55 ps) ESD time at pH 7.

It is interesting to note that this scenario implies that besides R82 also D212 might not belong to the minimal set of amino acids that are crucial for a wt-like pK_a of D85 and hence for the fast ESD dynamics at physiological pH. Indications for this come from results on R82Q/D212N.[39] It was shown that this double mutant shows partial recovery of wt properties including proton transport.

The results on the double mutant indicate that the mechanism that keeps D85 deprotonated at physiological pH does not require a positive charge at position 82. On the other hand, a positive charge at position 82 does not necessarily lead to a deprotonated D85 around pH 7 at 15 mM KCl (cp. Materials and methods). This is demonstrated by the results on R82C−Hg^+, which belongs to the blue forms at pH 5.8 (cp. Table 2). In Figure 4 the kinetics at 480 nm of R82C−Hg^+ (at pH 5.8) are shown together with those of deionized wt and wt at pH 7 for comparison. It can be concluded that the protonation state of D85 and thus the ESD behavior critically depends on the specific location of a positive charge at position 82, as determined by the length of the respective amino acid residue (R82 or R82C−Hg^+).

As can be seen from Table 2, besides the short ESD time (τ_1) a second component (τ_2) with significant amplitude is found in the blue forms. In general a number of explanations can be found for the appearance of more than one ESD component. Most likely is the existence of two electronic ground state isomers of the retinal cofactor,[40,41] but other scenarios such as a branching of the reaction path in the excited electronic state as suggested for the biphasic ESD in halorhodopsin[42,43] are possible.

Further inspection of Tables 1 and 2 shows that the distribution of the observed ESD times τ_1 around their respective mean values of 0.52 ± 0.05 and 1.7 ± 0.3 ps is rather narrow whereas the longer ESD time (τ_2) shows stronger variations (roughly 6−12 ps), even among the R82 mutants. This is in agreement with other results described in the literature.[23,44] The robustness of the observed ESD times τ_1 with respect to sample modifications of different chemical nature, either mutations or variation of pH or ion concentration, again confirms D85 as the carrier of the dominating charge governing the ESD time τ_1. On the other hand, the relative insensitivity of τ_1 and the sensitivity of τ_2 with respect to chemical changes indicate that two different reaction mechanisms must be involved.

In conclusion, we have shown that the set of charged amino acid residues in the binding pocket of the retinal cofactor in bacteriorhodopsin that affect the fast photoisomerization must be distinguished from the minimal set that is crucial, i.e., essential for it. In fact, the results show that in the double mutant R82A/G231C at pH 7 R82 is not necessary for the fast decay of the excited electronic state of ≈0.5 ps although in the single mutant R82A the excited-state decay is slowed. In this sense, R82 does not belong to the crucial binding pocket. It remains an open question as to whether the space of parameters defining the crucial binding pocket can be reduced further. An approach for its better characterization is given by those double mutant proteins that are revertants concerning the primary photoreaction, photocycle, and biological activity, such as R82A/G231C.

Acknowledgment. We thank D. Stehlik and M. P. Heyn for support and encouragement. This work was partly supported by DFG (Di 405/5-1,2 and Sfb 312/B1). We thank I. Wallat for technical assistance.

References and Notes

(1) For reviews about retinal proteins see: *Isr. J. Chem.* **1995**, *35* (3−4).

(2) Oesterhelt, D.; Stoeckenius, W. *Nature New Biol.* **1971**, *233*, 149.

(3) Stoeckenius, W.; Bogomolni, R. A. *Annu. Rev. Biochemistry* **1982**, *21*, 587.

(4) Ebrey, T. G. *Thermodynamics of Membrane Receptors and Channels*; Jackson, M., Ed.; CRC Press: Boca Raton, FL, 1993; p 353.
(5) Nuss, M. C.; Zinth, W.; Kaiser, W.; Kölling, E.; Oesterhelt, D. *Chem. Phys. Lett.* **1985**, *117*, 1.
(6) Mathies, R. A.; Brito Cruz, C. H.; Pollard, W. T.; Shank, C. V. *Science* **1988**, *240*, 777.
(7) Schneider, G.; Diller, R.; Stockburger, M. *Chem. Phys.* **1989**, *131*, 17.
(8) Govindjee, R.; Balashov, S. P.; Ebrey, T. G. *Biophys. J.* **1990**, *58*, 597.
(9) Xie, A. *Biophys. J.* **1990**, *58*, 1127.
(10) Doig, S. J.; Reid, P. J.; Mathies, R. A. *J. Phys. Chem.* **1991**, *95*, 6372.
(11) Brack, T. L.; Atkinson, G. H. *J. Phys. Chem.* **1991**, *95*, 2351.
(12) Diller, R.; Maiti, S.; Walker, G. C.; Cowen, B. R.; Pippenger, R.; Bogomolni, R. A.; Hochstrasser, R. M. *Chem. Phys. Lett.* **1995**, *241*, 109.
(13) Diller, R. *Chem. Phys. Lett.* **1998**, *295*, 47.
(14) Aton, B.; Doukas, A. G.; Callendar, R. H.; Becher, B.; Ebrey, T. G. *Biochemistry* **1977**, *16*, 2995.
(15) Stockburger, M.; Klusmann, W.; Gattermann, H.; Massig, G.; Peters, R. *Biochemistry* **1979**, *18*, 4886.
(16) Fodor, S. P. A.; Ames, J. B.; Gebhard, R.; van den Berg, E. M. M.; Stoeckenius, W.; Lugtenburg, J.; Matthies, R. A. *Biochemistry* **1988**, *27*, 7097.
(17) Hasson, K. C.; Gai, F.; Anfinrud, P. A. *Proc. Natl. Acad. Sci. U.S.A.* **1996**, *93*, 15124.
(18) Haran, G.; Wynne, K.; Xie, A.; He, Q.; Chance, M.; Hochstrasser, R. M. *Chem. Phys. Lett.* **1996**, *261*, 389.
(19) Zhong, Q.; Ruhman, S.; Ottolenghi, M.; Sheves, M.; Friedman, N.; Atkinson, G. H.; Delaney, J. K. *J. Am. Chem. Soc.* **1996**, *118*, 12828.
(20) Song, L.; El-Sayed, M. A. *J. Am. Chem. Soc.* **1998**, *120*, 8889.
(21) Hamm, P.; Zurek, M.; Röschinger, T.; Patzelt, H.; Oesterhelt, D.; Zinth, W. *Chem. Phys. Lett.* **1996**, *263*, 613.
(22) Kobayashi, T.; Terauchi, M.; Kouyama, T.; Yoshizawa, M.; Taiji, M. *SPIE Laser Appl. Life Sci.* **1990,** *1403*, 407.
(23) Song, L.; El-Sayed, M. A.; Lanyi, J. K. *Science* **1993**, *261*, 891.
(24) Subramaniam, S.; Marti, T.; Khorana, H. G. *Proc. Natl. Acad. Sci. U.S.A.* **1990**, *87*, 1013.
(25) Otto, H.; Marti, T.; Holz, M.; Mogi, T.; Stern, L. J.; Engel, F.; Khorana, H. G.; Heyn, M. P. *Proc. Natl. Acad. Sci. U.S.A.* **1990**, *87*, 1018.
(26) Alexiev, U.; Mollaaghababa, R.; Khorana, H. G.; Heyn, M. P. *J. Biol. Chem.* **2000**, *275*, 13431.
(27) Krebs, M. P.; Mollaaghababa, R.; Khorana, H. G. *Proc. Natl. Acad. Sci. U.S.A.* **1993**, *90*, 1987.
(28) Alexiev, U.; Mollaaghababa, R.; Scherrer, P.; Khorana, H. G.; Heyn, M. P. *Proc. Natl. Acad. Sci. U.S.A.* **1995**, *92*, 372.
(29) Alexiev, U.; et al. Unpublished results.
(30) Metz, G.; Siebert, F.; Engelhard, M. *FEBS Lett.* **1992**, *203*, 237.
(31) Humphrey, W.; Bamberg, E.; Schulten, K. *Biophys. J.* **1997**, *72*, 1347.
(32) Warshel, A.; Chu, Z. T.; Hwang, J.-K. *Chem. Phys.* **1991**, *158*, 304.
(33) Garavelli, M.; Celani, P.; Bernardi, F.; Robb, M. A.; Olivucci, M. *J. Am. Chem. Soc.* **1997**, *119*, 6891.
(34) Braiman, M. S.; Mogi, T.; Marti, T.; Stern, L. J.; Khorana, H. G.; Rothschild, K. J. *Biochemistry* **1988**, *27*, 8516.
(35) Brown, L. S.; Bonet, L.; Needleman, R.; Lanyi, J. K. *Biophys. J.* **1993**, *65*, 124.
(36) Grigorieff, N.; Ceska, T. A.; Downing, K. H.; Baldwin, J. M.; Henderson, R. *J. Mol. Biol.* **1996**, *259*, 393.
(37) Pebay-Peyroula, E.; Rummel, G.; Rosenbusch, J. P.; Landau, E. M. *Science* **1997**, *277*, 1677.
(38) Luecke, H.; Richter, H. T.; Lanyi, J. K. *Science* **1998**, *280*, 1934.
(39) Brown, L.; Váró, G.; Hatanaka, M.; Sasaki, J.; Kandori, H.; Maeda, A.; Friedman, N.; Sheves, M.; Needleman, R.; Lanyi, J. *Biochemistry* **1995**, *34*, 12903.
(40) Logunov, S. L.; Masciangioli, T. M.; El-Sayed, M. A. *J. Phys. Chem. B* **1998**, *102*, 8109.
(41) Song, L.; Yang, D.; El-Sayed, M. A. Lanyi, J. K. *J. Phys. Chem.* **1995**, *99*, 10052.
(42) Arlt, T.; Schmidt, S.; Zinth, W.; Haupts, U.; Oesterhelt, D. *Chem. Phys. Lett.* **1995**, *241*, 559.
(43) Kandori, H.; Yoshihara, K.; Tomioka, H.; Sasabe, H. *J. Phys. Chem.* **1992**, *96*, 6066.
(44) Logunov, S. L.; El-Sayed, M. A.; Song, L.; Lanyi, J. K. *J. Phys. Chem.* **1996**, *100*, 2391.
(45) Abbreviations: bR, bacteriorhodopsin; hR, halorhodopsin; wt, wild type; ESD, excited-state decay; R82A (Q, C), mutant with arginine in position 82 replaced by alanine (glutamine, cysteine); R82A/G231C, double mutant with arginine in position 82 replaced by alanine and glycine in position 231 replaced by cysteine.